Preprints of the 19th World Congress
The International Federation of Automatic Control
Cape Town, South Africa. August 24-29, 2014

Voltage and Angle Stability Reserve of Power Systems with Renewable Generation

Ulrich Münz * **Michael Metzger** *

* *Siemens Corporate Technology, Otto-Hahn-Ring 6, 81739 Munich, Germany (e-mail: {ulrich.muenz,michael.metzger}@siemens.com).*

Abstract: Voltage and angle stability of power systems with renewable power supply and the corresponding region of attraction are analyzed jointly. First, the power system model is derived that consists of algebraic power network equations and differential power generator equations. The renewable power generators like photovoltaic inverters or wind turbines are modeled with first order dynamics. Second, power system stability is analyzed for two kinds of power networks: high-voltage networks with purely inductive power lines and medium-/low-voltage networks with homogeneous resistive-inductive power lines. For both cases, decoupling droop controllers are presented and the stability of this power system including these controllers is analyzed. The analysis is based on contraction arguments that have been used before to prove consensus in multi-agent system. However, due to the particular structure of the power system model, conventional contraction arguments have to be adapted for this analysis.

Keywords: Power systems, voltage stability, angle stability, contraction.

1. INTRODUCTION

The interconnection of neighboring power systems has led to improved system security and economy of operation. These benefits have been recognized from the beginning, and thus interconnections have grown continuously. The result are very large systems of enormous complexity (Kundur, 1993). For example, the synchronous grid of Continental Europe covers most countries of Continental Europe as well as some countries in Africa and Asia. The massive integration of fluctuating renewable energy sources like wind and solar power into these power systems lead to new challenges for power system analysis and design, cf. Schaber et al. (2012). This integration of renewable sources and the vulnerability of critical infrastructures like power grids to natural disasters and terrorist attacks has brought up the idea of a microgrid. A microgrid is an integrated energy system consisting of distributed energy resources (DER) and multiple electrical loads operating as a single, autonomous grid. It can be operated either in parallel to or "islanded" from the existing utility power grid. Microgrids are usually operated at low or medium voltage. This has impact to the grid stability and controller design, as discussed below.

Today, power system analysis is usually based on nonlinear simulations and – wherever possible – linear analysis around a stable equilibrium. Controller design for power systems is often based on experience and verification in simulations. This design works fine if the worst case behavior is described accurately by a limited number of simulations and operation points. However, if the worst case behavior is more complex, e.g. because of quickly fluctuating power flows, this design becomes more and more cumbersome. This becomes particularly challenging if large amounts of renewable and fluctuating energy sources like wind and solar power are supplying the power system because, in this case, the power generation and power flows can change abruptly. Therefore, it is desirable to use analytical conditions instead of simulations for power system analysis and design.

In this paper, we provide analytical conditions on the voltage and angle stability reserve of a power system with renewable generation, i.e. the stability and the region of attraction of its steady state. First, the power system model is derived. It consists of first order power generator models that describe renewable generators like photovoltaic (PV) and wind turbines (WT), and battery storage (BS) that are connected to the grid via converters. The generators are controlled by proportional droop controllers. The power network is modeled by highly nonlinear static equations that describe the relation between the voltage amplitude and phase at each bus (node) on the one hand and the active and reactive power supply and consumption at each bus (node) on the other hand. We derive these equations for both high-voltage (HV) power networks with purely inductive power lines and medium-/low-voltage (MV/LV) power networks with resistive-inductive power lines. At each bus, exactly one generator is connected to the grid. The resulting model has two states for each bus, voltage amplitude and phase, and a quite complex nested interconnection between the states of each buses. The derivation and suitable re-writing of this model is one contribution of this paper. In the second part of the paper, we determine the steady state of this power system as well as its stability and region of attraction for both HV and MV/LV networks. The proof is based on a contraction argument similar to Lin (2006). Yet, previous results have to be suitably adapted in order to be applied to the nested interconnection of the power system. This is the main contribution of this paper.

Angle stability analysis of power systems has been described, e.g., in Dörfler and Bullo (2012b); Münz and Romeres (2013); Schiffer et al. (2013a). Voltage stability has been analyzed among others in Dib et al. (2009a,b) based on detailed differential-algebraic power system models under the assumption that the power system has an infinitely strong swing bus with predefined voltage amplitude and phase. Here, we do not require such an assumption. To the best of our knowledge, joint voltage and angle stability analysis conditions have so far only been derived in Wang et al. (2013); Schiffer et al. (2013b). Yet, both publications do not provide a region of attraction. Up to date, the stability reserve, i.e. the region of attraction, is determined numerically for specific power system parameters, see Sauer and Pai (2006) for an overview. Here, we provide an analytical condition on the region of attraction.

We first describe and explain the appropriate power system model in Section 2. Then, we derive conditions for stability and the region of attraction for HV power systems in Section 3. Finally, we extend these results to MV/LV power systems in Section 4. The paper is concluded in Section 5.

2. POWER SYSTEMS MODELING

2.1 Single Power Line Model

The power line between bus (or node) i and j is described by a concentrated parameter model containing a series interconnection of a resistance $r_{ij} = r_{ji}$ and an inductance $l_{ij} = l_{ji}$. The capacitors at each end of the power line are neglected here. This is possible if either the power lines are short or if they are considered as concentrated capacitors at each bus, e.g. Kundur (1993); Sauer and Pai (2006).

We concentrate here on voltage and angle stability but not on fast subtransients in the power grid. Therefore, we neglect transients in the power lines and assume that voltages and currents are roughly sinosoidal with approximately nominal frequency. Under this assumption, all voltages and currents can be described in a rotating frame that rotates with the nominal grid frequency f_N, e.g. 50 Hz or 60 Hz. Hence, all voltages $\underline{u}_i$ are parameterized fully by their amplitude u_i and their phase θ_i. This allows to describe the static power line model in the complex domain with a constant complex impedance $\underline{z}_{ji} = \underline{z}_{ij} = r_{ij} + \jmath\omega_0 l_{ij} = r_{ij} + \jmath x_{ij} = z_{ij}e^{\jmath\phi_{ij}}$, where $\jmath^2 = -1, \omega_0 = 2\pi f_N, x_{ij} = \omega_0 l_{ij} = x_{ji} > 0, z_{ij} > 0, \phi_{ij} \in [0, \frac{\pi}{2}]$. The voltages at bus i and j are $\underline{u}_i = u_i e^{\jmath\theta_i}$ and $\underline{u}_j = u_j e^{\jmath\theta_j}$, where $u_i, u_j, \theta_i, \theta_j$ are time-varying quantities.

The apparent, active, and reactive power, $\underline{s}_{ij}, p_{ij}, q_{ij}$, fed into the power line at the end i is

$$\begin{aligned}\underline{s}_{ij} = p_{ij} + \jmath q_{ij} = \underline{u}_i \underline{i}_{ij}^* &= \underline{u}_i \left(\frac{\underline{u}_i - \underline{u}_j}{\underline{z}_{ij}}\right)^* \\ &= u_i \frac{u_i - u_j e^{-\jmath(\theta_j - \theta_i)}}{r_{ji} - \jmath x_{ji}} \\ &= \frac{(r_{ji} + \jmath x_{ji})u_i}{r_{ji}^2 + x_{ji}^2} \left(u_i - u_j(\cos\theta_{ij} + \jmath \sin\theta_{ij})\right).\end{aligned}$$

where $\theta_{ij} = \theta_i - \theta_j$. We separate the apparent power into active and reactive power and obtain

$$p_{ij} = \frac{u_i}{r_{ij}^2 + x_{ij}^2} \left(r_{ij}(u_i - u_j \cos\theta_{ij}) + x_{ij} u_j \sin\theta_{ij}\right), \quad (1)$$

$$q_{ij} = \frac{u_i}{r_{ij}^2 + x_{ij}^2} \left(x_{ij}(u_i - u_j \cos\theta_{ij}) - r_{ij} u_j \sin\theta_{ij}\right). \quad (2)$$

2.2 Power Network Model

We set up a model for a complete power network with N buses (or nodes). We define a bus set $\mathcal{N} = \{1, \dots, N\}$. The set $\mathcal{N}_i$ with $N_i = |\mathcal{N}_i|$ is the set of all buses $j \in \mathcal{N}$ that are connected to bus i by a power line.

The power conservation law implies that all active p_i and all reactive q_i power supplied to the power network at one bus i has to equal the sum of all active and reactive power leaving this bus to one of its neighbors $j \in \mathcal{N}_i$, i.e.

$$p_i = \sum_{j \in \mathcal{N}_i} p_{ij}, \qquad q_i = \sum_{j \in \mathcal{N}_i} q_{ij}. \quad (3)$$

Note that $\frac{r_{ij}}{r_{ij}^2 + x_{ij}^2} = \frac{r_{ij}}{z_{ij}^2} = \frac{\cos\phi_{ij}}{z_{ij}}$ and $\frac{x_{ij}}{r_{ij}^2 + x_{ij}^2} = \frac{x_{ij}}{z_{ij}^2} = \frac{\sin\phi_{ij}}{z_{ij}}$. Thus, we have with (1) and (2)

$$\begin{pmatrix} p_i \\ q_i \end{pmatrix} = \sum_{j \in \mathcal{N}_i} \frac{u_i}{z_{ij}} \begin{pmatrix} \sin\phi_{ij} & \cos\phi_{ij} \\ -\cos\phi_{ij} & \sin\phi_{ij} \end{pmatrix} \begin{pmatrix} u_j \sin\theta_{ij} \\ u_i - u_j \cos\theta_{ij} \end{pmatrix}.$$

Note that the matrix depending on ϕ_{ij} is a rotation matrix that degenerates into the identity matrix for purely inductive lines, i.e. with $r_{ij} = 0$ and therefore $\phi_{ji} = \frac{\pi}{2}$.

We introduce the following assumption:

Assumption 1. (Homogeneous power lines). *We assume that the impedances $\underline{z}_{ij}, i, j, \in \mathcal{N}$, of all power lines of the power network satisfy $\underline{z}_{ij} = z_{ij}e^{\jmath\phi}, z_{ij} > 0, \phi \in [0, \frac{\pi}{2}]$, with identical angle ϕ for all lines.*

This assumption can be easily justified. If all power lines in the grid are of the same type, their $\frac{r_{ij}}{x_{ij}}$ ratios are identical, whereas the actual r_{ij} and x_{ij} values depend on the power line length. Hence, all ϕ_{ij} are identical but the power line length may still be different and is reflected in $\underline{z}_{ij}$.

With this assumption, we obtain

$$\begin{pmatrix} p_i \\ q_i \end{pmatrix} = \begin{pmatrix} \sin\phi & \cos\phi \\ -\cos\phi & \sin\phi \end{pmatrix} \sum_{j \in \mathcal{N}_i} \frac{u_i}{z_{ij}} \begin{pmatrix} u_j \sin\theta_{ij} \\ u_i - u_j \cos\theta_{ij} \end{pmatrix}. \quad (4)$$

2.3 Droop Controlled Power Converters

All generated power is supplied to the network with converters, e.g. photovoltaic inverters, wind turbine with full converter, or battery inverters. In order to achieve stability, several converters are grid forming inverters as described below. Non-grid-forming converters can be modeled in a similar way but are left out here for page restrictions.

Grid forming converters provide a defined voltage $\underline{u}_i$ to the grid depending on active power p_i and reactive power q_i measurements. For a three phase power system, we may assume instantaneous but noisy active and reactive power measurements. The voltage amplitude u_i and angle θ_i are determined by proportional controllers, called *droop* controllers,

$$\dot{\theta}_i = \omega_0 - k_{pi}(p_i - p_{i0}) \quad (5)$$

$$u_i = u_{i0} - k_{qi}(q_i - q_{i0}), \quad (6)$$

where p_{i0}, p_{i0}, and u_{i0} are the predefined active and reactive power and voltage set-points of node i and ω_0 is the nominal frequency of the power network. The droop parameters k_{pi} and k_{qi} are all strictly positive.

The voltage phase following (5) has some filtering property to active power measurements noise. For the voltage amplitude, we add an additional first-order low-pass filter to damp reactive power measurement noise and obtain

$$\dot{u}_i = -\tilde{k}_{qi}\left((u_i - u_{i0}) + k_{qi}(q_i - q_{i0})\right). \quad (7)$$

After all, we have

$$\begin{pmatrix} \dot{\theta}_i \\ \frac{1}{\tilde{k}_{qi}} \dot{u}_i \end{pmatrix} = \begin{pmatrix} \omega_0 \\ -(u_i - u_{i0}) \end{pmatrix} - K_i \begin{pmatrix} p_i - p_{i0} \\ q_i - q_{i0} \end{pmatrix}, \quad (8)$$

where $K_i = \mathrm{diag}(k_{pi}, k_{qi})$. Later on, we will also use a non-diagonal *droop matrix* K_i

$$K_i = \begin{pmatrix} k_{pi} & 0 \\ 0 & k_{qi} \end{pmatrix} \begin{pmatrix} \sin\phi & -\cos\phi \\ \cos\phi & \sin\phi \end{pmatrix}, \quad (9)$$

for some rotation angle ϕ.

2.4 Passive Loads

Passive loads are modeled as active and/or reactive power consumption. First of all, all loads [1] that are connected to buses without generators are shifted to buses with generators using Kron reduction techniques, see for example Dörfler and Bullo (2012a). As a consequence, there is a generator at each bus of the reduced power system. Then, the loads at bus i are modeled by subtracting the corresponding active and reactive power consumption from the value p_{i0}, q_{i0} of the generator at this bus in (8). For ease of notation, we do not introduce an additional parameter for p_{i0}, q_{i0} but stick to these parameters having in mind that they also include local passive loads.

2.5 Power System Modeling

Connecting (4) and (8), we obtain the power system model

$$\begin{pmatrix}\dot\theta_i\\ \dot u_i\end{pmatrix} = \begin{pmatrix}\omega_0\\ -\tilde k_{qi}(u_i-u_{i0})\end{pmatrix} + \begin{pmatrix}1 & 0\\ 0 & \tilde k_{qi}\end{pmatrix} K_i \left(\begin{pmatrix}p_{i0}\\ q_{i0}\end{pmatrix} - \sum_{j\in\mathcal{N}_i} \frac{u_i}{z_{ij}} \begin{pmatrix}\sin\phi & \cos\phi\\ -\cos\phi & \sin\phi\end{pmatrix} \begin{pmatrix}u_j\sin\theta_{ij}\\ u_i - u_j\cos\theta_{ij}\end{pmatrix}\right), \quad (10)$$

that is analyzed in the rest of the paper. A similar model is investigated in Wang et al. (2013).

3. STABILITY ANALYSIS OF HV POWER SYSTEM

We consider here first the simpler case with purely inductive power lines, i.e. $r_{ij} = 0$ for all i, j and therefore $\phi = \frac{\pi}{2}$. This simplification will be relaxed in Section 4. In this case, the power system model (10) simplifies to

$$\begin{pmatrix}\dot\theta_i\\ \dot u_i\end{pmatrix} = \begin{pmatrix}\omega_0\\ -\tilde k_{qi}(u_i-u_{i0})\end{pmatrix} + \begin{pmatrix}1 & 0\\ 0 & \tilde k_{qi}\end{pmatrix} K_i \times \left(\begin{pmatrix}p_{i0}\\ q_{i0}\end{pmatrix} - \sum_{j\in\mathcal{N}_i} \frac{u_i}{z_{ij}} \begin{pmatrix}u_j\sin\theta_{ij}\\ u_i - u_j\cos\theta_{ij}\end{pmatrix}\right). \quad (11)$$

Note that the phase dynamics show some Kuramoto-like behavior for constant voltages u_i, u_j. Moreover, the voltage dynamics show some contracting behavior for constant phase differences θ_{ij}. The main challenge here is to prove that the coupled dynamics also converge to a steady state.

3.1 Transformation to Steady State

First, we investigate the steady states of the power grid model (11). We start our investigation with the phase dynamics. Therefore, we introduce the following coordinate transformation

$$\theta_i(t) = \Omega t + \vartheta_i^* + \vartheta_i(t), \quad (12)$$

where Ω is the steady state frequency, i.e. $\lim_{t\to\infty}\dot\theta_i(t) = \Omega$, and ϑ_i^* describes the relative steady state phase differences, i.e. $\lim_{t\to\infty}(\theta_i - \theta_j) = \vartheta_i^* - \vartheta_j^*$. These limits exist under the conditions following later on.

We use (12) to rewrite (11) as

$$\begin{pmatrix}\dot\vartheta_i\\ \dot u_i\end{pmatrix} = \begin{pmatrix}\omega_0-\Omega\\ -\tilde k_{qi}(u_i-u_{i0})\end{pmatrix} + \begin{pmatrix}1 & 0\\ 0 & \tilde k_{qi}\end{pmatrix} K_i \times \left(\begin{pmatrix}p_{i0}\\ q_{i0}\end{pmatrix} - \sum_{j\in\mathcal{N}_i} \frac{u_i}{z_{ij}} \begin{pmatrix}u_j\sin(\vartheta_{ij}+\vartheta_{ij}^*)\\ u_i - u_j\cos(\vartheta_{ij}+\vartheta_{ij}^*)\end{pmatrix}\right), \quad (13)$$

where $\vartheta_{ij} = \vartheta_i - \vartheta_j$ and $\vartheta_{ij}^* = \vartheta_i^* - \vartheta_j^*$.

We analyze the steady state of these differential equations, i.e. $\dot\vartheta = 0, \dot u_i = 0$. In steady state, we have $\vartheta_i - \vartheta_j = 0$ for all i, j and the steady state equation simplifies to

$$0 = \begin{pmatrix}\omega_0-\Omega\\ -\tilde k_{qi}(u_i^*-u_{i0})\end{pmatrix} + \begin{pmatrix}1 & 0\\ 0 & \tilde k_{qi}\end{pmatrix} K_i \times \left(\begin{pmatrix}p_{i0}\\ q_{i0}\end{pmatrix} - \sum_{j\in\mathcal{N}_i} \frac{u_i^*}{z_{ij}} \begin{pmatrix}u_j^*\sin\vartheta_{ij}^*\\ u_i^* - u_j^*\cos\vartheta_{ij}^*\end{pmatrix}\right). \quad (14)$$

These equations for $i \in \mathcal{N}$ define the steady state $(\Omega, u^*, \vartheta^*)$ of the power grid. For given ω_0, $u_0 = \mathrm{vec}(u_{i0})$, $p_0 = \mathrm{vec}(p_{i0})$, $q_0 = \mathrm{vec}(q_{i0})$, K_i, and $\tilde k_q$ (with $\mathrm{vec}(\chi_i)$ the vector of χ_i), they provide a set of $2N$ equations with $2N$ unknowns $u_1^*, \dots, u_N^*, \vartheta_1^* - \vartheta_2^*, \vartheta_2^* - \vartheta_3^*, \dots, \vartheta_{N-1}^* - \vartheta_N^*, \Omega$.

We assume now that $\omega_0, u_0, p_0, q_0, K_i$, and $\tilde k_q$ are chosen such that a solution of (14) exists. The existence of such a solution is obviously a necessary condition for the existence of a stable power grid behavior. Then, we define the following bounds

$$\Delta\vartheta^* = \max_{i,j}|\vartheta_i^* - \vartheta_j^*| = \|B^T\vartheta^*\|_\infty, \quad (15)$$

$$\Delta u^* = \max_{i,j}|u_i^* - u_j^*| = \|B^T u^*\|_\infty, \quad (16)$$

where B is the incidence matrix of the power network topology and $\vartheta^* = \mathrm{vec}(\vartheta_i^*), u^* = \mathrm{vec}(u_i^*)$. Clearly, both $\Delta\vartheta^*$ and Δu^* depend on $\omega_0, u_0, p_0, q_0, K_i$, and $\tilde k_q$.

We subtract (14) from (13) and obtain with $\tilde u_i = u_i - u_i^*$

$$\begin{aligned}\begin{pmatrix}\dot\vartheta_i\\ \dot{\tilde u}_i\end{pmatrix} &= \begin{pmatrix}0\\ -\tilde k_{qi}\tilde u_i\end{pmatrix} - \begin{pmatrix}1 & 0\\ 0 & \tilde k_{qi}\end{pmatrix} K_i \sum_{j\in\mathcal{N}_i}\frac{1}{z_{ij}} \\ &\times \begin{pmatrix}u_iu_j\sin(\vartheta_{ij}+\vartheta_{ij}^*) - u_i^*u_j^*\sin(\vartheta_{ij}^*)\\ u_i^2 - u_i^{*2} - u_iu_j\cos(\vartheta_{ij}+\vartheta_{ij}^*) + u_i^*u_j^*\cos(\vartheta_{ij}^*)\end{pmatrix} \\ &= \begin{pmatrix}0\\ -\tilde k_{qi}\tilde u_i\end{pmatrix} - \begin{pmatrix}1 & 0\\ 0 & \tilde k_{qi}\end{pmatrix} K_i \sum_{j\in\mathcal{N}_i}\frac{1}{z_{ij}} \\ &\times \left[\begin{pmatrix}(u_i\tilde u_j + u_j^*\tilde u_i)\sin(\vartheta_{ij}+\vartheta_{ij}^*)\\ (u_i+u_i^*)\tilde u_i - (u_i\tilde u_j + u_j^*\tilde u_i)\cos(\vartheta_{ij}+\vartheta_{ij}^*)\end{pmatrix}\right. \\ &\left. + \begin{pmatrix}u_i^*u_j^*\left(\sin(\vartheta_{ij}+\vartheta_{ij}^*) - \sin(\vartheta_{ij}^*)\right)\\ -u_i^*u_j^*\left(\cos(\vartheta_{ij}+\vartheta_{ij}^*) - \cos(\vartheta_{ij}^*)\right)\end{pmatrix}\right], \end{aligned} \quad (17)$$

where we use $u_i^2 - u_i^{*2} = (u_i + u_i^*)\tilde u_i$ and $u_iu_j - u_i^*u_j^* = u_i\tilde u_j + u_j^*\tilde u_i$.

Note that the phase dynamics of (17) consist of a locally passive coupling term $\sin(\vartheta_{ij}+\vartheta_{ij}^*) - \sin(\vartheta_{ij}^*)$ with constant gain $u_i^*u_j^*$ and another term $(u_i\tilde u_j + u_j^*\tilde u_i)\sin(\vartheta_{ij}+\vartheta_{ij}^*)$ that has to be dominated by the coupling. The voltage dynamics consist of damping terms $\tilde k_{qi}\tilde u_i$, $(u_i+u_i^*)\tilde u_i$, and other terms $(u_i\tilde u_j + u_j^*\tilde u_i)\cos(\vartheta_{ij}+\vartheta_{ij}^*)$ and $u_i^*u_j^*\left(\cos(\vartheta_{ij}+\vartheta_{ij}^*) - \cos(\vartheta_{ij}^*)\right)$ that again need to be dominated.

3.2 Contraction Analysis

Now, we prove the convergence of the power system (17), i.e. $\lim_{t\to\infty}\vartheta_{ij} = 0$ and $\lim_{t\to\infty}\tilde u_i = 0$, for suitable initial

[1] The Kron reduction is only feasible for constant impedance and constant current loads. Therefore, we exclude constant power loads in our setup to avoid algebraic loops. A relaxation of this restriction is future work.

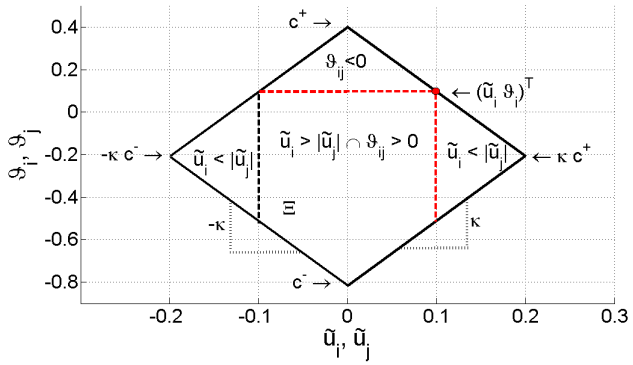

Fig. 1. Exemplary set Ξ (18) and exemplary subsystem state $(\tilde{u}_i, \vartheta_i)^T$ with corresponding subsets $\tilde{u}_i < |\tilde{u}_j|$, $\vartheta_{ij} < 0$, and $\tilde{u}_i > |\tilde{u}_j| \cap \vartheta_{ij} > 0$.

conditions and under suitable conditions on the parameters $\tilde{k}_{qi} > 0, k_{pi} > 0, k_{qi} > 0, z_{ij} = z_{ji} > 0, u_i^* > 0, u_j^* > 0, \vartheta_{ij}^*$, where the last parameters are actually derived from the steady state equation (14). The proof is based on a contraction analysis, e.g. Lin (2006). Contraction analysis typically considers time-varying hyper-rectangles in the state space aligned with coordinate axis that contain all states of all subsystems. Then, contraction arguments are used to prove that this rectangle is positively invariant and eventually contracts to a single point. Here, it is not clear how to show contraction of a rectangular set in the $\tilde{u}_i, \vartheta_i$ state space because of the complicated non-contracting terms in (17). Instead of a rectangular set, we propose to use a diamond shape convex set $\Xi(\kappa, t)$ depending on the parameter $\kappa > 0$ and defined by two inequality constraints

$$\Xi(t) = \Big\{ (x_1, x_2) \in \mathbb{R}^2 : x_2 \leq -\frac{1}{\kappa}|x_1| + c^+(t), \text{ and } x_2 \geq \frac{1}{\kappa}|x_1| - c^-(t) \Big\}, \quad (18)$$

where $c^+(t), c^-(t)$ are defined as

$$c^+(t) = \max_i(\vartheta_i(t) + \frac{1}{\kappa}|\tilde{u}_i(t)|) \quad (19)$$

$$c^-(t) = \min_i(\vartheta_i(t) - \frac{1}{\kappa}|\tilde{u}_i(t)|). \quad (20)$$

This set Ξ is illustrated in Figure 1.

Note that $\Xi(t)$ contains the states $\vartheta_i(t), \tilde{u}_i(t)$ of all agents for any time t. Therefore, we have

$$|\vartheta_i(t) - \vartheta_j(t)| \leq c^+(t) - c^-(t), \quad (21)$$

$$|\tilde{u}_i(t) - \tilde{u}_j(t)| \leq \kappa(c^+(t) - c^-(t)), \quad (22)$$

$$|\tilde{u}_i(t)| \leq \frac{\kappa}{2}(c^+(t) - c^-(t)), \quad (23)$$

for all i, j and all $t \geq 0$. Below, we provide conditions such that Ξ is non-increasing, i.e. Ξ defines a positively invariant set. Moreover, we show that Ξ contracts to a single point, i.e. $\lim_{t\to\infty}(c^+(t) - c^-(t)) = 0$.

Vector Flow on the Boundary of Ξ In order to prove that Ξ is positively invariant, we show that the vector field $(\dot{\vartheta}_i \ \dot{\tilde{u}}_i)^T$ on the boundary $\partial\Xi$ of Ξ is pointing towards the interior of the diamond. As the boundary $\partial\Xi$ is not smooth, we have to investigate the four boundary parts individually. Due to page limitations, we only describe here the upper right boundary. The other three boundaries can be derived similarly.

In all cases, we consider the following inner product

$$\begin{pmatrix} 1 & \frac{1}{\pm\kappa} \end{pmatrix} \begin{pmatrix} \dot{\vartheta}_i \\ \dot{\tilde{u}}_i \end{pmatrix}, \quad (24)$$

where the sign in front of κ is positive on the upper right and lower left boundary and negative on the upper left and lower right boundary, respectively. This inner product has to be negative in the upper boundaries and positive on the lower boundaries. With $k_{qi}^* = \frac{\tilde{k}_{qi}}{\kappa} k_{qi}$, we compute

$$\begin{aligned}
\begin{pmatrix} 1 & \frac{1}{\kappa} \end{pmatrix} \begin{pmatrix} \dot{\vartheta}_i \\ \dot{\tilde{u}}_i \end{pmatrix} &= -\frac{\tilde{k}_{qi}}{\kappa}\tilde{u}_i - \sum_{j\in\mathcal{N}_i} \frac{1}{z_{ij}} \begin{pmatrix} k_{pi} & k_{qi}^* \end{pmatrix} \\
&\times \left[\begin{pmatrix} (u_i\tilde{u}_j + u_j^*\tilde{u}_i)\sin(\vartheta_{ij} + \vartheta_{ij}^*) \\ (u_i + u_i^*)\tilde{u}_i - (u_i\tilde{u}_j + u_j^*\tilde{u}_i)\cos(\vartheta_{ij} + \vartheta_{ij}^*) \end{pmatrix} \right. \\
&\left. + \begin{pmatrix} u_i^*u_j^*\left(\sin(\vartheta_{ij} + \vartheta_{ij}^*) - \sin(\vartheta_{ij}^*)\right) \\ -u_i^*u_j^*\left(\cos(\vartheta_{ij} + \vartheta_{ij}^*) - \cos(\vartheta_{ij}^*)\right) \end{pmatrix} \right] \\
&= -\frac{\tilde{k}_{qi}}{\kappa}\tilde{u}_i - \sum_{j\in\mathcal{N}_i} \frac{1}{z_{ij}} \left[k_{qi}^*(u_i + u_i^*)\tilde{u}_i \right. \\
&- \left(k_{qi}^*\cos(\vartheta_{ij} + \vartheta_{ij}^*) - k_{pi}\sin(\vartheta_{ij} + \vartheta_{ij}^*)\right) \\
&\times (u_i\tilde{u}_j + u_j^*\tilde{u}_i) \\
&+ \left[k_{pi}(\sin(\vartheta_{ij} + \vartheta_{ij}^*) - \sin(\vartheta_{ij}^*)) \right. \\
&\left.\left. -k_{qi}^*(\cos(\vartheta_{ij} + \vartheta_{ij}^*) - \cos(\vartheta_{ij}^*))\right] u_i^*u_j^* \right].
\end{aligned}$$

Using trigonometric identities, we obtain $k_{qi}^*\cos(\vartheta_{ij} + \vartheta_{ij}^*) - k_{pi}\sin(\vartheta_{ij} + \vartheta_{ij}^*) = k_i^*\sin(-\vartheta_{ij} - \vartheta_{ij}^* + \tilde{k}_i^*)$,where $k_i^* = \sqrt{k_{pi}^2 + \frac{\tilde{k}_{qi}^2 k_{qi}^2}{\kappa^2}}$ and the sign of $\tilde{k}_i^* = \arctan\frac{\tilde{k}_{qi}k_{qi}}{\kappa k_{pi}}$ depends on the sign of κ. Moreover, we have $k_{qi}^*(\cos(\vartheta_{ij} + \vartheta_{ij}^*) - \cos(\vartheta_{ij}^*)) + k_{pi}(\sin(\vartheta_{ij} + \vartheta_{ij}^*) - \sin(\vartheta_{ij}^*))$
$= 2\sin\frac{\vartheta_{ij}}{2}(k_{qi}^*\sin(\vartheta_{ij}^* + \frac{\vartheta_{ij}}{2}) + k_{pi}\cos(\vartheta_{ij}^* + \frac{\vartheta_{ij}}{2})) = 2\sin\frac{\vartheta_{ij}}{2}k_i^*\cos(\vartheta_{ij}^* + \frac{\vartheta_{ij}}{2} - \tilde{k}_i^*)$.The cosine function $\cos(\vartheta_{ij}^* + \frac{\vartheta_{ij}}{2} - \tilde{k}_i^*)$ is positive if

$$\vartheta_{ij} \in \left(\pi - 2|\tilde{k}_i^*| - 2\Delta\vartheta^* - \epsilon\right)[-1, 1], \quad (25)$$

where $\Delta\vartheta^*$ is defined in (15) and $\epsilon > 0$ guarantees that $\cos\left(\vartheta_{ij}^* + \frac{\vartheta_{ij}}{2} - \tilde{k}_i^*\right) > \sin\epsilon$. This condition is satisfied if

$$c^+(0) - c^-(0) \leq \pi - 2\arctan\frac{\tilde{k}_{qi}k_{qi}}{|\kappa|k_{pi}} - 2\Delta\vartheta^* - \epsilon \quad (26)$$

holds, see (21). In summary, we have

$$\begin{aligned}
\begin{pmatrix} 1 & \frac{1}{\kappa} \end{pmatrix} \begin{pmatrix} \dot{\vartheta}_i \\ \dot{\tilde{u}}_i \end{pmatrix} &= -\frac{\tilde{k}_{qi}}{\kappa}\tilde{u}_i + \sum_{j\in\mathcal{N}_i} \frac{1}{z_{ij}} \left[-k_{qi}^*(u_i + u_i^*)\tilde{u}_i \right. \\
&+ k_i^*\sin\left(-\vartheta_{ij} - \vartheta_{ij}^* + \tilde{k}_i^*\right)(u_i\tilde{u}_j + u_j^*\tilde{u}_i) \\
&\left. -2k_i^*u_i^*u_j^*\sin\frac{\vartheta_{ij}}{2}\cos\left(\vartheta_{ij}^* + \frac{\vartheta_{ij}}{2} - \tilde{k}_i^*\right)\right]. \quad (27)
\end{aligned}$$

Now, we consider the upper right boundary and some agent i on this boundary with $\vartheta_i + \frac{1}{\kappa}\tilde{u}_i = c^+$. The vector field $(\dot{\vartheta}_i \ \dot{\tilde{u}}_i)^T$ is pointing toward the interior of Ξ if

$$\begin{pmatrix} 1 & \frac{1}{\kappa} \end{pmatrix} \begin{pmatrix} \dot{\vartheta}_i \\ \dot{\tilde{u}}_i \end{pmatrix} < 0. \quad (28)$$

In order to prove this, we have to consider the influence of each j in the summation of all neighbors independently. We separate Ξ in three subsets depending on the location of agent i on the boundary and its neighbor j, see Figure 1:

(i) $\tilde{u}_i < |\tilde{u}_j|$, (ii) $\vartheta_{ij} < 0$, and (iii) $\tilde{u}_i \geq |\tilde{u}_j|$ and $\vartheta_{ij} \geq 0$. Recall that we have an additional information due to the fact that we consider only the vector flow of agent i on the upper right boundary, i.e. $\tilde{u}_i + \kappa\vartheta_i \geq |\tilde{u}_j| + \kappa\vartheta_j$, that can be rewritten as

$$-\vartheta_{ij} \leq \frac{\tilde{u}_i - |\tilde{u}_j|}{\kappa}. \tag{29}$$

3.2.1.1. Case $\tilde{u}_i < |\tilde{u}_j|$ Note that the boundary condition (29) implies that $-\vartheta_{ij}$ decreases as $\tilde{u}_i - |\tilde{u}_j|$ decreases. Moreover, $\tilde{u}_i < |\tilde{u}_j|$ implies $\vartheta_{ij} > 0$. This implies the sinus in the last summand of (27) can be bounded as

$$-\sin\frac{\vartheta_{ij}}{2} \leq \sin\left(\frac{\tilde{u}_i - |\tilde{u}_j|}{2\kappa}\right) \leq \operatorname{sinc}\left(\frac{c^+ - c^-}{2}\right)\frac{\tilde{u}_i - |\tilde{u}_j|}{2\kappa},$$

where $\operatorname{sinc}(x) = \frac{\sin(x)}{x}$. Thus, we have with ϵ from (26)

$$\begin{aligned}
&-k^*_{qi}(u_i+u^*_i)\tilde{u}_i + k^*_i \sin\left(-\vartheta_{ij} - \vartheta^*_{ij} + \tilde{k}^*_i\right)(u_i\tilde{u}_j + u^*_j\tilde{u}_i) \\
&\quad - 2k^*_i u^*_i u^*_j \sin\frac{\vartheta_{ij}}{2}\cos\left(\vartheta^*_{ij} + \frac{\vartheta_{ij}}{2} - \tilde{k}^*_i\right) \\
&\leq -k^*_{qi}(u_i+u^*_i)\tilde{u}_i + k^*_i \sin\left(-\vartheta_{ij} - \vartheta^*_{ij} + \tilde{k}^*_i\right)(u_i\tilde{u}_j + u^*_j\tilde{u}_i) \\
&\quad + u^*_i u^*_j k^*_i \sin\epsilon \operatorname{sinc}\left(\frac{c^+ - c^-}{2}\right)\frac{\tilde{u}_i - |\tilde{u}_j|}{\kappa} \\
&= \Big[-k^*_{qi}(u_i + u^*_i) + k^*_i \sin\left(-\vartheta_{ij} - \vartheta^*_{ij} + \tilde{k}^*_i\right) u^*_j \\
&\quad + \frac{u^*_i u^*_j}{\kappa} k^*_i \sin\epsilon \operatorname{sinc}\left(\frac{c^+ - c^-}{2}\right)\Big]\tilde{u}_i \\
&\quad + k^*_i \Big[\sin\left(-\vartheta_{ij} - \vartheta^*_{ij} + \tilde{k}^*_i\right) u_i \\
&\quad - \frac{u^*_i u^*_j}{\kappa}\sin\epsilon \operatorname{sinc}\left(\frac{c^+ - c^-}{2}\right)\operatorname{sign}(\tilde{u}_j)\Big]\tilde{u}_j,
\end{aligned}$$

where $\operatorname{sign}(\cdot)$ is the signum function. As $\tilde{u}_i \geq 0$ can be arbitrarily small compared to $\tilde{u}_j > \tilde{u}_i$, we impose

$$\frac{u^*_j u^*_i}{\kappa}\sin\epsilon \operatorname{sinc}\frac{c^+ - c^-}{2} > u_i, \tag{30}$$

which guarantees that the last term including $\tilde{u}_j$ is negative. We relax this condition using $u_i = u^*_i + \tilde{u}_i$ and (23) to

$$\frac{u^*_j}{\kappa}\sin\epsilon \operatorname{sinc}\frac{c^+ - c^-}{2} > 1 + \frac{\kappa(c^+ - c^-)}{2u^*_i}. \tag{31}$$

With (31), we have

$$\begin{aligned}
&-k^*_{qi}(u_i+u^*_i)\tilde{u}_i + k^*_i \sin\left(-\vartheta_{ij} - \vartheta^*_{ij} + \tilde{k}^*_i\right)(u_i\tilde{u}_j + u^*_j\tilde{u}_i) \\
&\quad - 2k^*_i u^*_i u^*_j \sin\frac{\vartheta_{ij}}{2}\cos\left(\vartheta^*_{ij} + \frac{\vartheta_{ij}}{2} - \tilde{k}^*_i\right) \\
&\leq \Big[-k^*_{qi}(u_i + u^*_i) + k^*_i \sin\left(-\vartheta_{ij} - \vartheta^*_{ij} + \tilde{k}^*_i\right) u^*_j \\
&\quad + \frac{u^*_i u^*_j}{\kappa} k^*_i \sin\epsilon \operatorname{sinc}\left(\frac{c^+ - c^-}{2}\right)\Big]\tilde{u}_i \\
&\leq -\left(k^*_{qi}(u_i + u^*_i) - \left(1 + \frac{u^*_i}{\kappa}\right) u^*_j k^*_i\right)\tilde{u}_i.
\end{aligned} \tag{32}$$

We continue with (32) after considering the other cases.

3.2.1.2. Case $\vartheta_{ij} < 0$ Note that this implies $\tilde{u}_i > |\tilde{u}_j|$, see Figure 1. In this case, the last summand of (27) is positive because of (26) and $\vartheta_{ij} < 0$. Yet, it is bounded because of (26) and (29) as

$$-\sin\frac{\vartheta_{ij}}{2}\cos\left(\vartheta^*_{ij} + \frac{\vartheta_{ij}}{2} - \tilde{k}^*_i\right) \leq \sin\frac{\tilde{u}_i - \tilde{u}_j}{2\kappa} \leq \frac{\tilde{u}_i - \tilde{u}_j}{2\kappa}.$$

Thus, we have

$$\begin{aligned}
&-k^*_{qi}(u_i+u^*_i)\tilde{u}_i + k^*_i \sin\left(-\vartheta_{ij} - \vartheta^*_{ij} + \tilde{k}^*_i\right)(u_i\tilde{u}_j + u^*_j\tilde{u}_i) \\
&\quad - 2k^*_i u^*_i u^*_j \sin\frac{\vartheta_{ij}}{2}\cos\left(\vartheta^*_{ij} + \frac{\vartheta_{ij}}{2} - \tilde{k}^*_i\right) \\
&\leq -k^*_{qi}(u_i+u^*_i)\tilde{u}_i + k^*_i \sin\left(-\vartheta_{ij} - \vartheta^*_{ij} + \tilde{k}^*_i\right)(u_i\tilde{u}_j + u^*_j\tilde{u}_i) \\
&\quad + \frac{u^*_i u^*_j}{\kappa} k^*_i(\tilde{u}_i - \tilde{u}_j) \\
&\leq -\left(k^*_{qi}(u_i + u^*_i) - k^*_i\left(u^*_j + u_i + \frac{2u^*_i u^*_j}{\kappa}\right)\right)\tilde{u}_i,
\end{aligned} \tag{33}$$

because $|\tilde{u}_j| \leq \tilde{u}_i$.

3.2.1.3. Case $\tilde{u}_i \geq |\tilde{u}_j|$ and $\vartheta_{ij} \geq 0$ This time, (26) guarantees that the last summand of (27) is non-positive because $\vartheta_{ij} \geq 0$. Thus, we have

$$\begin{aligned}
&-k^*_{qi}(u_i+u^*_i)\tilde{u}_i + k^*_i \sin\left(-\vartheta_{ij} - \vartheta^*_{ij} + \tilde{k}^*_i\right)(u_i\tilde{u}_j + u^*_j\tilde{u}_i) \\
&\quad - 2k^*_i u^*_i u^*_j \sin\frac{\vartheta_{ij}}{2}\cos\left(\vartheta^*_{ij} + \frac{\vartheta_{ij}}{2} - \tilde{k}^*_i\right) \\
&\leq -\left(k^*_{qi}(u_i + u^*_i) + k^*_i(u^*_j + u_i)\right)\tilde{u}_i,
\end{aligned} \tag{34}$$

where we use $|\tilde{u}_j| \leq \tilde{u}_i$.

3.2.1.4. Collecting all three cases Summarizing the three cases (32), (33), and (34), we have

$$\begin{aligned}
&\begin{pmatrix}1 & \frac{1}{\kappa}\end{pmatrix}\begin{pmatrix}\dot{\vartheta}_i \\ \dot{\tilde{u}}_i\end{pmatrix} \leq -\frac{\tilde{k}_{qi}}{\kappa}\tilde{u}_i - \sum_{j\in\mathcal{N}_i}\frac{1}{z_{ij}} \\
&\times\left(\frac{\tilde{k}_{qi}}{\kappa}k_{qi}(u_i + u^*_i) - k^*_i\left(u^*_j + u_i + \frac{2u^*_i u^*_j}{\kappa}\right)\right)\tilde{u}_i,
\end{aligned} \tag{35}$$

given that (26) and (31) hold.

Hence, $\begin{pmatrix}1 & \frac{1}{\kappa}\end{pmatrix}\begin{pmatrix}\dot{\vartheta}_i \\ \dot{\tilde{u}}_i\end{pmatrix} < 0$ holds if for all $i \in \mathcal{N}$

$$\begin{aligned}
&\frac{\tilde{k}_{qi}}{\kappa}\Big(1 + \sum_{j\in\mathcal{N}_i}\frac{k_{qi}u^*_i}{z_{ij}}\Big) \\
&\quad > \sum_{j\in\mathcal{N}_i}\frac{1}{z_{ij}}\Bigg[\sqrt{k^2_{pi} + \frac{\tilde{k}^2_{qi}k^2_{qi}}{\kappa^2}}\left(u^*_j + \frac{2u^*_i u^*_j}{\kappa}\right) \\
&\quad + \sqrt{k^2_{pi} + \frac{\tilde{k}^2_{qi}k^2_{qi}}{\kappa^2}} - \frac{\tilde{k}_{qi}k_{qi}}{\kappa}\left(u^*_i + \frac{\kappa}{2}(c^+ - c^-)\right)\Bigg]
\end{aligned} \tag{36}$$

is satisfied, where we used $|u_i| \leq u^*_i + \frac{\kappa}{2}(c^+ - c^-)$.

The same conditions are obtained for the other three boundaries. They are left out here for page limitations.

Contraction of Ξ Summarizing our calculations up to this point, we have shown that conditions (26), (31), and (36) guarantee that the vector field $\begin{pmatrix}\dot{\vartheta}_i & \dot{\tilde{u}}_i\end{pmatrix}^T$ on the boundary $\partial\Xi$ is directed toward the interior of Ξ. Hence,

the convex set Ξ is positively invariant. It remains to show that Ξ is in fact contracting to a single point.

We prove the contraction of Ξ using a Barbalat argument (Khalil, 2002) for $\Delta c(t) = c^+(t) - c^-(t)$. Note that $\lim_{t\to\infty} \Delta c(t) - \Delta c(0) = \int_0^\infty \Delta c(\tau) d\tau$In this case, $\dot{c}^+(t) - \dot{c}^-(t)$ is non-positive and the integral is finite because $c^+ - c^-$ is non-increasing and bounded from below by zero. The derivative of $\dot{c}^+ - \dot{c}^-$, i.e. the second derivative of $c^+ - c^-$, is bounded because derivatives of $\dot{\tilde{u}}_i$ and $\dot{\vartheta}_i$ are bounded. Thus, we have $\lim_{t\to\infty} \dot{c}^+(t) - \dot{c}^-(t) = 0$. In other words, as time goes to infinity, the set Ξ stops contracting.

Finally, we have to show that Ξ only stops contracting if it is a single point. The set Ξ stops contracting if a subsystem i on the boundary $\partial\Xi$ stays at the boundary, i.e. $\begin{pmatrix} 1 & \frac{1}{\kappa} \end{pmatrix} \begin{pmatrix} \dot{\vartheta}_i \\ \dot{\tilde{u}}_i \end{pmatrix} = 0$ or $\begin{pmatrix} 1 & -\frac{1}{\kappa} \end{pmatrix} \begin{pmatrix} \dot{\vartheta}_i \\ \dot{\tilde{u}}_i \end{pmatrix} = 0$ depending on the boundary. Going back to Equation (35), we see that the above equality requires $\tilde{u}_i = 0$. This means that the agent, that stays on the boundary, has to satisfy $\lim_{t\to\infty} \tilde{u}_i(t) = 0$. If we have another look at (35), we see that this equality also requires $\tilde{u}_j = 0$ for all neighboring j of subsystem i with $\tilde{u}_j > \tilde{u}_i = 0$. Hence, we may conclude that $\lim_{t\to\infty} \tilde{u}_i(t) = 0$ for all $i \in \mathcal{N}$. This also implies $\lim_{t\to\infty} \dot{\tilde{u}}_i(t) = 0$ for all $i \in \mathcal{N}$. Replacing $\tilde{u}_i = \tilde{u}_j = \dot{\tilde{u}}_i = 0$ in (17), we obtain $0 = \sum_{j\in\mathcal{N}_i} \frac{1}{z_{ij}} u_j^* (\cos(\vartheta_{ij} + \vartheta_{ij}^*) - \cos(\vartheta_{ij}^*))$,which is true for all $i \in \mathcal{N}$ only if $\vartheta_{ij} = 0$ for all $i, j \in \mathcal{N}$. This implies $\lim_{t\to\infty} \vartheta_{ij}(t) = 0$ for all $i, j \in \mathcal{N}$. Hence, Ξ contracts to a single point.

3.3 Main Result

We summarize these derivations in the following theorem

Theorem 2. Given a HV power system (11) with steady state (14). This steady state is asymptotically attracting for all initial conditions in Ξ if (26), (31), and (36) hold.

4. STABILITY ANALYSIS OF MV/LV POWER SYSTEMS

Now, we consider a distribution network with nonzero resistance, i.e. $r_{ij} \gg 0$ and $0 \leq \phi_{ij} \ll \frac{\pi}{2}$. We assume that the power lines are homogenous, i.e. Assumption 1 holds and we have $\phi_{ij} = \phi$ for all i, j.

We go back to (4) and suggest to rotate the droop controller (8) using (9). Such a rotation of the droop controller has previously been suggested in De Brabandere et al. (2004) for a single inverter connected to an infinte bus. Here, we extend this concept to large power systems with interconnected renewable generation. This way, we obtain again decoupled dynamics for phase and voltage and Theorem 2 can directly be extended to this case:

Corollary 3. Given a MV/LV power system (10) with homogeneous power lines satisfying Assumption 1 and a power system droop controller (8) with decoupling gain (9) with steady state given by (14). This steady state is asymptotically attracting for all initial conditions in Ξ if Conditions (26), (31), and (36) hold.

5. CONCLUSIONS

We derived a power system model that describes both voltage and angle dynamics of a power system with converter coupled power generation, which is the case for most renewable sources. Stability is achieved by standard droop controllers for purely inductive HV power lines, e.g. in transmission networks, and by a decoupling droop controller for resistive-inductive MV/LV power lines, e.g. in distribution networks. The latter is particularly important for stability analysis and controller design for microgrids. Stability is proven using a contraction argument used previously to prove consensus in multi-agent systems. Yet, previous results had to be suitably adapted in order to be applicable to the nested interaction between voltage and angle dynamics. The system setup excluding rotating masses results in a first order system which enables contraction arguments to prove synchronization. This also indicates that the dominance of power electronic converters in distributed generation does not necessarily deteriorate grid stability. Future work should focus on the incorporation of conventional generators with rotating masses that require at least second order angle dynamics at the buses.

REFERENCES

De Brabandere, K., Bolsens, B., Van den Keybus, J., Woyte, A., Driesen, J., and Belmans, R. (2004). A voltage and frequency droop control method for parallel inverters. In *Proc. 35th annual IEEE Power Electronics Specialists Conference*, 2501 – 2507.

Dib, W., Ortega, R., Barabanov, A., and Lamnabhi-Lagarrigue, F. (2009a). A globally convergent controller for multi-machine power systems using structure-preserving models. *IEEE Trans. Autom. Control*, 54(9), 2179–2185.

Dib, W., Ortega, R., Hill, D., and Lamnabhi-Lagarrigue, F. (2009b). Nonlinear excitation control for transient stability of multi-machine power systems using structure-preserving models. In *6th IFAC Symp. Power Plants and Power System control*.

Dörfler, F. and Bullo, F. (2012). Synchronization and transient stability in power networks and non-uniform Kuramoto oscillators. *SIAM Journal on Control and Optimization*, 50(3), 1616–1642.

Dörfler, F. and Bullo, F. (2013). Kron reduction of graphs with applications to electrical networks. *IEEE Trans. Circuits and Systems I: Regular Papers*, 60(1), 150–163.

Khalil, H.K. (2002). *Nonlinear Systems*. Prentice Hall, Upper Saddle River, NJ, 3rd edition.

Kundur, P. (1993). *Power System Stability and Control*. McGraw-Hill.

Lin, Z. (2006). *Coupled Dynamic Systems: From Structure towards Stability and Stabilizability*. Ph.D. thesis, University of Toronto, Canada.

Münz, U. and Romeres, D. (2013). Region of attraction of power systems. In *Proc. 4th IFAC Workshop on Estimation and Control of Networked Systems*. Koblenz, Germany.

Sauer, P.W. and Pai, M.A. (2006). *Power System Dynamics and Stability*. Stipes Publishing L.L.C.

Schaber, K., Steinke, F., Mühlich, P., and Hamacher, T. (2012). Parametric study of variable renewable energy integration in europe: Advantages and costs of transmission grid extensions. *Energy Policy*, 42, 498–508.

Schiffer, J., Goldin, D., Raisch, J., and Sezi, T. (2013a). Synchronization of droop-controlled microgrids with distributed rotational and electronic generation. In *IEEE Conf. Dec. Contr.*

Schiffer, J., Ortega, R., Astolfi, A., Raisch, J., and Sezi, T. (2013b). Conditions for stability of droop-controlled inverter-based microgrids. submitted.

Wang, Z., Xia, M., and Lemmon, M. (2013). Voltage stability of weak power distribution networks with inverter connected sources. In *Proc. American Control Conference*, 6577–6582.